DRAFT

2/9/92

IN-33

372774

3178MS00.DOC

Traveling-Wave Tubes

Carol L. Kory

ANALEX Corporation
NASA Lewis Research Center, M. S. 54-5
21000 Brookpark Road
Cleveland, Ohio 44135

The traveling-wave tube (TWT) is a vacuum device invented in the early 1940's (1, 2) used for amplification at microwave frequencies. Amplification is attained by surrendering kinetic energy from an electron beam to a radio frequency (RF) electromagnetic wave. The demand for vacuum devices has been decreased largely by the advent of solid-state devices. However, although solid state devices have replaced vacuum devices in many areas, there are still many applications such as radar, electronic countermeasures and satellite communications, that require operating characteristics such as high power (Watts to Megawatts), high frequency (below 1 GHz to over 100 GHz) and large bandwidth that only vacuum devices can provide. Vacuum devices are also deemed irreplaceable in the music industry where musicians treasure their tube-based amplifiers claiming that the solid-state and digital counterparts could never provide the same "warmth" (3). The term traveling-wave tube includes both fast-wave and slow-wave devices. This article will concentrate on slow-wave devices as the vast majority of TWTs in operation fall into this category.

TWT Principle Components

The TWT possesses four major components as shown in Figure 1(4):
(1) An electron gun which produces an electron beam
(2) A slow-wave circuit which slows an RF electromagnetic wave to a speed synchronous with the electron beam
(3) A collector which collects the spent electron beam
(4) The TWT package providing cooling, beam focusing, and access to the RF input and output
Amplification is obtained by feeding the RF signal to be amplified into the slow-wave circuit while the electron beam is moving along the TWT axis. The slow-wave structure reduces the electromagnetic wave phase velocity so that it propagates near synchronism with the electron beam resulting in interaction between the wave and the beam, and thus amplification of the RF signal. The spent electron beam is collected at the end of the tube by the collector.

Electron Gun

The electron gun is used to produce the electron beam. The electron guns used for nearly all TWTss mimic a section of spherical diode as first derived by Pierce (6), and are consequently referred to as Pierce guns. The major components of the gun are the cathode, heater, focus electrode and one or more anodes. The type of cathode used in TWTs is the thermionic cathode where electron emission is achieved by using a heat source to supply the electrons near the surface of the cathode with enough energy to escape from the surface. Cathode operation is a complex subject and the reader can consult (17) or the chapter on cathodes in this publication for further detail. In a simplified description, the higher the temperature of the cathode, the greater the emission (current density), but the shorter the life. Because of the limited lifetime of cathodes, the electron gun design must be consistent with the expected life of the application. For example, if a lifetime of 12 to 15 years is required, as in commercial space applications, cathode current densities of 1 A/cm^2 or less are usually specified for an M-type cathode (8).

A heater connected to a dc or ac power supply, consisting of a coil of tungsten or tungsten-rhenium wire adjacent to or embedded within the cathode body is typically used to raise the

temperature of the cathode to an adequate level for electron emission. The wire is formed into a contrawound coil to reduce the amount of magnetic field introduced into the electron gun by the current through the heater, thus reducing large perturbations in the electron trajectories which would make the beam difficult to focus or couple modulation onto the electron beam.

The anode is a positively charged electrode which attracts and accelerates the electrons emitted from the cathode. Because of electrostatic repulsion forces, the electrons are deflected as they are emitted so the focus electrode is used to produce equipotential lines with the same center of curvature as the cathode resulting in electron flow toward this center of curvature; therefore, the electrons are focused into a beam. TWTs used in pulse applications often have a grid placed close to the cathode which permits the electron beam to be turned off and on with a small swing (relative to the cathode-to-ground potential drop) in the applied grid-to-cathode bias. The grid causes some perturbation of the beam so it is typically not used in high reliability devices.

Slow-Wave Circuit

The RF voltage to be amplified is fed into the slow-wave circuit through the input coupler. The purpose of the slow-wave circuit is to slow down the axial velocity of the RF wave so that it propagates near synchronism with the electron beam. There are numerous possible slow-wave circuits limited only by human inventiveness. Some of the more commonly used structures include helix, contrawound helix, coupled-cavity, ring-bar, clover-leaf, ladder and grating circuits. The axial component of the electric field set up by the voltage on the circuit is somewhat sinusoidal in the vicinity of the electron beam so a force is directed to the left when the field is positive and to the right when the field is negative (See Figure 1). This causes some of the electrons in the beam to decelerate (force is directed to the left) and others to accelerate (force is directed to the right) causing the electron beam to form bunches, or be velocity modulated. The bunches drift into a decelerating region of the field and the electrons lose velocity and thus kinetic energy. The energy lost by the electrons is transferred to RF energy in the RF wave, thus amplifying the RF signal. Further down the length of the tube, the bunch becomes more compact leaving even more electrons in the decelerating region causing the RF wave to grow even more. As this continues, the electron velocities decrease and space charge forces within the bunch increase. Eventually a portion of the bunch leaves the decelerating region of the circuit field and enters the accelerating region. These electrons extract energy from the circuit field. When the energy extracted from the circuit field becomes equal to the energy supplied, amplification of the RF wave stops and the interaction is said to reach saturation.

Backward wave oscillations (BWOs) occur when power is reflected back to the input because of a mismatch in the slow-wave circuit, at the load or at the output coupler. Because of a mismatch at the input, a portion of the signal is again reflected to provide a feedback signal. To prevent these reflections, or backward waves, from reaching the input, it is common that a sever or distributed loss is added to the slow-wave circuit. A sever isolates the input wave from the output wave by physically separating the sections. Distributed loss usually consists of a lossy resistive coating which attenuates both forward and backward waves. Although the RF wave is severed or attenuated at this point in the slow-wave circuit, the bunching of the electrons has

been established and will reestablish the RF wave on the circuit beyond the sever or region of attenuation, allowing interaction to continue.

A common method to increase efficiency by prolonging synchronism between the electron beam and the RF wave is to incorporate a velocity taper in the TWT design. A velocity taper is achieved by changing the dimensions of the slow-wave circuit near the output of the tube so that the RF wave velocity is slowed along with the electron beam. With this technique, even though the electron bunches are slowed as they lose energy to the circuit, they will remain in synchronism longer with the consecutively slowed RF wave and continue to deliver energy to the circuit fields. Velocity tapering has proved to significantly increase the efficiency of TWT's (9, 10 and 11). In addition, the technique can be used to enhance the linearity of the power output versus power input (12) and to prevent BWOs (13, 14 and 15).

Helix

The helix is the most common type of slow-wave structure. A typical modern helical structure embodies a metal tape wound into a helix supported by three or more dielectric support rods inside a conducting barrel. Figure 2 shows the cross-sectional view of a typical helical circuit and a three-dimensional view of the helical tape. Derived from a single-wire transmission line which has zero dispersion, the helix has a primarily constant phase velocity over a large bandwidth making it the widest bandwidth circuit of any structure available. This relatively low dispersion can be reduced further by incorporating dispersion shaping techniques into the circuit design. This is achieved by perturbing the circuit fields predominantly at low frequencies so that the phase velocity is decreased at the low frequency end while staying constant at high frequencies, thus reducing dispersion and increasing bandwidth. Since the fields are concentrated between the helical turns at high frequencies and in the area extending from the helix to the barrel at low frequencies, this low frequency perturbation is possible by including specially shaped dielectric support rods or longitudinally conducting metal vanes which anisotropically load the circuit (16 and 17). Several loading methods are shown in Figure 3.

Coupled-Cavity Circuit

Another common slow-wave structure is the coupled-cavity circuit which is used mostly for high-power applications. Because of its all metal construction, it is able to dissipate a greater amount of heat compared to the helix, but can operate over only a comparatively narrow bandwidth. As shown in Figure 4 for the cross-sectional and top views, the circuit includes a chain of cavities, typically made of copper, brazed together with a coupling slot alternating 180 degrees at adjacent cavities. Ferrules surround the beam hole to concentrate the RF electric field in the vicinity of the electron beam for increased interaction.

Collector

After the amplified RF output is removed from the TWT the spent electron beam passes through the end of the beam focusing section, so space charge forces cause the beam to expand as it enters the collector. Upon entering the collector, the beam is highly disordered with a broad

spectrum of energies. The electron beam at this point still possesses a great deal of kinetic energy as only about 10 to 30 percent is extracted during interaction with the RF wave (19). If the collector were at the same potential as the body of the tube, this kinetic energy would be dissipated as heat on the collector surface. By operating the collector electrode at a potential below that of the RF circuit, the beam is decelerated before it hits the collector surface. Thus, some of the remaining kinetic energy from the electron beam is converted to electric potential energy. This negative potential operation is known as depressing the collector. The greater the amount of recovered power, the higher the total efficiency of the tube. The impact of an efficient collector is made clear by considering the efficiency formula. Overall efficiency can be expressed as the ratio of the output power to input power or

$$\eta_{ov} = \frac{P_{out}}{P_{in}} \quad (1)$$

where P_{out} is the RF power output and P_{in} is the sum of the heater power, P_h, beam power from the gun, P_o, RF input power, P_{RF}, and power to the magnetic focusing system, P_m, minus the power recovered by the collector, P_{rec}, or

$$P_{in} = P_h + P_o + P_m + P_{RF} - P_{rec} \; . \quad (2)$$

plots the current to the collector versus the amount by which the collector is depressed below ground potential (the slow-wave circuit potential). Assuming zero loss and zero interception between the beam and the slow-wave circuit, the area under the curve represents the maximum power that could possibly be recovered by the collector. The remaining area of the rectangle, or the area above the curve is the beam power converted to RF power. The beam current and voltage are represented by I_O and V_O, respectively. For a single stage collector depressed to voltage V_1, the maximum power that can be recovered is represented graphically in (a) by the shaded area which is the product of the magnitudes of the collector current and collector voltage or

$$P_{rec} = V_1 \, I_O \, .$$

Several phenomena complicate the collector operation including space charge effects of the electrons already in the collector repelling those electrons entering, secondary electron emission from the surface caused by striking electrons, and electrons having different amounts of kinetic energy, thus traveling with different velocities. Multistage depressed collectors (MDC), where several electrodes are used at different depressed potentials, incorporate multiple velocity sorting stages. This directs high velocity electrons to the stages having the greatest depression and the slow electrons to the stages with the least depression. This design has proven to greatly increase the overall efficiency of TWTs (20). The reason for this becomes clear when the collector current versus voltage curve is again considered for the multistage collector. The total possible recoverable power for an n stage MDC is represented by the shaded region in (b) where the nth electrode is at cathode potential, V_O. The possible recovered power is significantly greater compared to the single stage collector given as

$$P_{rec} = \sum_{k=1}^{n} V_k \, I_k \, .$$

Considering equations 1 and 2, it becomes obvious that the overall efficiency can be significantly increased. In practice, typical MDC designs incorporate no more than five collector stages as the law of diminishing returns starts to occur with regards to efficiency improvement versus design complexity. A typical azimuthally symmetric four-stage MDC design is shown in two-dimensions in Figure 1.

TWT Package

The TWT package serves as a mechanical support structure for the TWT and RF input/output connectors, a thermal path for the conduction of waste heat, an electromagnetic interference (EMI) shield and as a protective cover over the high voltage connections and beam focusing magnets (4).

Beam Focusing

The electrons in the beam each posses negative charge; therefore, they repel one another causing the beam to diverge. To counteract this space charge effect and prevent the beam from diverging and being intercepted by the slow-wave structure as it flows through the length of the tube, external focusing is applied using an axial magnetic field. One way of doing this is to surround the TWT with a large solenoid which can be a permanent magnet or an electromagnet. Because of their size and large amount of stray magnetic field, solenoids are typically used only on very high power (kW level) TWT's with high current density beams.

A more commonly used method for focusing is to employ periodic permanent magnet (PPM) focusing which is lighter and more compact than equivalent solenoidal magnets (21). Alternating iron pole pieces and cylindrical magnets are placed side by side along the length of the tube, the polarity of adjacent magnets being reversed as shown in . The PPM structure provides a nearly sinusoidal magnetic field at the beam axis with rms value about equal to the value of field required in a uniform field design.

Vacuum Envelope

It is necessary to operate the main components of the TWT under vacuum to ensure proper cathode operation and long cathode life, prevent formation of positive ions within the electron beam, and to avoid high voltage arcing at the electrodes. Thus, the gun, slow-wave structure and collector are contained in a leak tight vacuum envelope. The beam focusing mechanism is usually mounted outside of the vacuum envelope and this whole assembly is mounted in the TWT package.

Basic Field Theory

TWT gain is based on the surrender of energy from the electron beam to the RF electromagnetic wave. For this phenomena to occur the phase velocity of the RF wavel, v, must be in near synchronism with the dc beam velocity, u_o, or

$$v = u_o. \qquad (3)$$

The gain of the tube depends on the strength of this interaction. A summary of the small-signal analysis for TWT gain is summarized by Gewartowski in (22) and more succinctly by Wilson in (23), based on the analysis done by Pierce in (24). The theory neglects space harmonics of the RF field other than that which is synchronous with the electron beam assuming these harmonics have no net effect.

First, the equation is derived for the ac current induced on the beam by the RF field (electronic equation). Next, the RF field resulting from the modulated beam is derived (circuit equation). These equations are solved simultaneously to determine the self-consistent relations for the circuit and beam quantities. The equations take on a neater form when several parameters are defined. Pierce's small-signal gain parameter C is defined as

$$C^3 = \frac{K I_o}{4 V_o} \qquad (4)$$

where K is the interaction impedance defined as

$$K = \frac{\int |E|^2 dS}{2\beta^2 P S} \qquad (5)$$

where |E| is the magnitude of the RF axial electric field, $\beta = \omega/v$ is the axial propagation constant2, ω is the angular frequency ($2\pi f$), f is the frequency of operation, P is the total RF power flow and S is the cross-sectional surface area of the electron beam. I_o and V_o are the dc beam current and voltage, respectively. Pierce's space-charge parameter QC is defined as

$$QC = \frac{\omega_q^2}{4C^2\omega^2} \qquad (6)$$

where ω_q is the reduced plasma frequency.

---

1 The RF wave actually consists of space harmonics and the harmonic of interest must be in near synchronism with the dc beam velocity.

2 K, E and β are calculated for the space harmonic of interest.

A measure of synchronism between the electrons and the space harmonic wave is specified by Pierce's velocity parameter b defined as

$$b=\frac{u_o-v}{vC}. \qquad (7)$$

Pierce's loss parameter d is proportional to circuit attenuation and is defined as

$$d=\frac{\alpha\omega}{u_oC}. \qquad (8)$$

where α is the circuit attenuation including surface and attenuator losses. The various fields and beam quantities have a z dependence of the form

$$e^{-\Gamma z}$$

where Γ is the complex propagation constant for the circuit-beam coupled system. The allowed values for Γ are determined by simultaneously solving for the circuit and electronic equations. Doing so gives

$$\Gamma=j\frac{u_o}{\omega}(1+jC\delta). \quad (9)$$

Making the appropriate substitutions and taking advantage of the fact that C is small,

$$\delta^2=\frac{1}{-b+jd+j\delta}-4QC. \quad (10)$$

The solutions for Eq. (10) give three allowable propagation constants. Regardless of the values of d and QC, one will always obtain one growing wave which is responsible for the gain in the tube, one decaying wave, and one wave of nearly constant amplitude as long as the tube is operating near synchronism (small b).

The initial loss factor A_1 is defined as

$$A_1=20\log\left|\frac{\delta_1^2}{(\delta_1-\delta_2)(\delta_1-\delta_3)}\right| \ dB. \qquad (11)$$

The space-charge loss factor is defined as

$$A_2=20\log\left|\frac{\delta_1^2+4QC}{\delta_1^2}\right| \ dB. \ (12)$$

Next we define

$$B=54.6\mathrm{Re}(\delta_1) \qquad (13)$$

and the electronic wavelength number N as

$$N=\frac{u_o l}{2\pi\omega} \qquad (14)$$

where l is the length of the interaction circuit. The small-signal gain can now be expressed as

$$Gain_{s-s}=A_1+A_2+BCN-SEVER\ LOSS \ \ (dB) \quad (15)$$

where about 6 dB of loss is associated with each sever. It should be noted that the small-signal gain analysis is valid only when the tube is operating well below saturation. Near or at saturation, the TWT behaves in a non-linear manner and the small-signal theory is no longer valid.

TWT Computer Modeling

Because of the complexity of operation, there are numerous codes which are used in the design, development and analysis of TWT's. Some of the codes stand alone, others are incorporated into the Microwave and Millimeter-wave Advanced Computational Environment (MMACE) which is a vacuum electronics initiative directed at integrating existing codes into a compatible environment having a user friendly interface (25). A discussion of available codes follows which is grouped by TWT section. This section is intended to point the reader to the appropriate references for each code.

Electron Gun

Numerous codes exist which will calculate electron trajectories in electrostatic and magnetostatic focusing systems. EGUN is a widely used code which includes 2D fields and 3D particle trajectories (26). In contrast to EGUN's rectangular mesh capability, DEMEOS uses a deformable triangular mesh which is efficient in modeling both the small and relatively large dimensions of the electron gun (27). The two and one-half dimensional particle-in-cell (PIC) code MAGIC is also used in gun design (28). OOPIC is a C++ program designed to simulate the behavior of charged particles in a 2D geometry(29).

Slow-Wave Structure

There is a large variety of codes available for the analysis of slow-wave structures. An important step in TWT design is to obtain the cold-test characteristics of the circuit. Cold-testing implies testing the circuit or a scale model of the circuit on the RF test bench without the electron beam to obtain dispersion, interaction impedance and attenuation characteristics. Accurate results have been obtained in terms of cold-test parameters for several slow-wave circuits using codes like the three-dimensional (3D) electrodynamic PIC code MAFIA (30, 32), the 3D cold-test codes Micro-SOS (33, 36) and ARGUS/ESP of MMACE (37), the 3D cold-test code for helical structures TLM (38) and the 3D cold-test code limited to axially symmetric cavities in cylindrical coordinates SUPERFISH (39).

It is also important to obtain information about the match from the slow-wave structure to the input/output couplers. Accurate results regarding the transmission characteristics of TWT couplers have been obtained using codes like Ansoft Eminence (40) and MAFIA (41).

Collector

There has been significant progress made in the computational modeling of collectors within the past several years. Typically an electron trajectory code such as EGUN was used to aid in collector design (42), but because it can simulate only azimuthally symmetric structures with

steady-state electron streams, three-dimensional codes that compute instantaneous conditions are also being used. Several 3D codes have provided reasonably accurate results: the 3D PIC code, MAFIA (43); the 3D PIC collector simulator integrated into the MMACE framework, C3D (44); the 3D PIC code, PIC3D (45) and the 3D electron trajectory collector simulator, LKOBRA (46).

TWT Interaction

As mentioned previously, the field theory for small-signal gain provides insight into TWT interaction, but when the tube is operated near or at saturation, this analysis is no longer valid. Near saturation the TWT behaves in a non-linear manner referred to as large-signal operation. This means that when large-amplitude signals are present, higher order RF terms are no longer negligible as compared to the corresponding dc values. The analysis of the nonlinear system does not lend itself to neat solutions of closed form equations, so computational modeling becomes crucial (47). There are a number of codes available to simulate TWT interaction and thus provide characteristics such as gain, power transfer curves and efficiency near and at saturation.

There are several codes devoted strictly to helical TWT interaction such as the one-dimensional (1D) code which predicts intermodulation distortion CHRISTINE (48), the 2D code which incorporates 3D field vector components and beam velocities and which is part of the MMACE framework GATOR (49) and the 2D deformable disk model DDM HELIX TWT (50). The NASA CC TWT code analyzes interaction between a 3D electron beam and 2D RF electromagnetic fields in coupled-cavity TWT's (51). Fully three-dimensional PIC codes such as MAFIA, ARGUS, SOS and 3DPIC offer the advantage of being able to simulate an entire TWT section in 3D including modulation effects. Modeling the beam dynamics in just the TWT slow-wave section in 3D has been accomplished with good accuracy (52, 45) but an entire 3D TWT model from gun to collector has not yet been accomplished because of the computational intensity of the problem.

Future Trends

The microwave power module (MPM) is a recent development which has had a significant impact on microwave and millimeter-wave electronics system development by taking advantage of the benefits of both vacuum electronics and solid-state devices. The MPM is a lightweight, miniaturized RF amplifier consisting of a low noise, high-gain microwave monolithic integrated circuit (MMIC) preamplifier/signal conditioner, a high efficiency vacuum power booster TWT, and a miniaturized high efficiency integrated power conditioner. The MPM has proven to outperform conventional TWT technology in areas of power density (power per unit weight) and noise figure. Analyses also indicate improvement in reliability due to fewer components, lower typical operating temperatures and interconnection technology (53).

Once thought to be a declining field, there is now a substantial opportunity for growth in the commercial demand for TWT's. Particularly, two types of systems are of interest, satellite communications and local multipoint distribution systems (LMDS) (54). These commercial systems are close to turning the balance from a mostly military market to a commercial market. US industry is proposing to invest more than 35 billion dollars in commercial Ka-Band satellite

communications systems over the next six years. The LMDS concept would cover major metropolitan areas with a grid of cellular stations operating at Ka-Band and transmitting programming in competition with cable TV systems. One estimate suggests that 5,000 to 6,000 highly linear Ka-Band TWT's, probably operating at 28 GHz, would be required to implement LMDS in the continental US (55).

Figures

Figure 1 Basic TWT. The electron gun shown to the left encompasses the heater, cathode, focus electrode and anode. A multistage depressed collector is shown on the right with electron beam trajectories.

Figure 2 Cross-sectional view of typical helix slow-wave circuit and three-dimensional view of helical tape. The rectangular helical tape is supported by three rectangular dielectric support rods, all enclosed in a conducting barrel. The electron beam travels through the axial center (r=0) of the helical circuit.

Figure 3 Various dispersion shaping techniques for broadband helical TWTs. (a) a metal coating is applied to the dielectric support rods (b) the support rods are formed into T-shapes (c) loading vanes are added between the support rods.

Figure 4 (a) Cross-sectional view (b) Top view of ferruled coupled-cavity circuit. The coupled cavity circuit employs an all metal construction suitable for high power TWTs.

Figure 5 Collector current versus collector voltage. (a) The shaded area designates the maximum power which can be recovered by a single stage collector. (b) The shaded area designates the maximum power which can be recovered by a multistage depressed collector with n stages.(a) Cross-sectional view (b) Top view periodic permanent magnet focusing.

Bibliography

1 R. Kompfner, The invention of the traveling-wave tubes *IEEE Trans. Electron Devices,* Vol. ED-23, No. 7, pp. 730-738, 1976.

2 N. E. Lindenblad, U. S. Patent 2,3000,052 filed May 4, 1940, issued October 27, 1942.

3 R. Wilson, Digital be damned! These days, for high-end audio...—Vacuum tubes are aglow again, *Electronic Engineering Times*, Issue 909, July 8, 1996.

4. TWT/TWTA Handbook, Hughes Aircraft Company, Electron Dynamics Division, Torrance, CA, 1992.

5. TWT/TWTA Handbook, Hughes Aircraft Company, Electron Dynamics Division, Torrance, CA, 1992.

6 J. R. Pierce, *Theory and Design of Electron Guns*, 2nd ed. New York: Van Nostrand, 1954.

7 J. R. Pierce, *Theory and Design of Electron Guns*, 2nd ed. New York: Van Nostrand, 1954.

8 J. A. Dayton, Jr., Traveling-wave tube amplifier reliability, from 1995 IEEE MTT-S International Microwave Symposium/ TWTA Workshop Proc., May 1995.

9 A. N. Curren, R. W. Palmer, D. A. Force, L. Dombro and J. A. Long, High-efficiency helical traveling-wave tube with dynamic velocity taper and advanced multistage depressed collector, *IEEE Int. Electron Devices Meet. Tech. Dig.*, pp. 473-476, 1987.

10 J. D. Wilson, H. C. Limburg, J. A. Davis, I. Tammaru and J. P. Vaszari, A high efficiency ferruleless coupled-cavity traveling-wave tube with phase-adjusted taper, *IEEE Trans. Electron Devices,* Vol. ED-37, No. 12, pp. 2638-2643, 1990.

11 J. D. Wilson, A simulated annealing algorithm for optimizing RF power efficiency in coupled-cavity traveling-wave tubes, Accepted for publication in *IEEE Trans. On Electron Devices*, 1997.

12 H. G. Kosmahl and J. C. Peterson, A TWT amplifier with a linear power transfer characteristic and improved efficiency, NASA TM-83590, March 1984.

13 G. I. Haddad and R. M. Bevensee, Start-oscillation conditions of tapered backward-wave oscillators, *IEEE Trans. On Electron Devices*, ED-10, pp. 389-393, November 1963.

14 B. Epsztein and G. Kantrowicz, Suppression of backward-wave oscillations in multikilowatt helix TWT's, in *Proc. European Microwave Conf.*, pp. 376-380, September 1973.

15 K. Tsutaki, Y. Yuasa and Y. Morizumi, Numerical analysis and design for high-performance helix traveling-wave tubes, *IEEE Trans. Electron Devices,* Vol. ED-32, No. 9, pp. 1842-1849, 1985.

16 J. L. Putz and M. J. Cascone, Effective use of dispersion shaping in broadband helix TWT circuits, *IEEE Int. Electron Devices Meet. Tech. Dig.*, pp. 422-424, 1979.

17 A. S. Gilmour, Jr., *Principles of Traveling-Wave Tubes,* Norwood, MA: Artech House, 1994, pp. 328-329.

18 H. G. Kosmahl, Modern multistage depressed collectors - A review, *Proc. IEEE Trans. Electron Devices*, Vol. 70, No. 11, pp.1325-1334, 1982.

19 J. W. Hansen, System Aspects of Communications TWTA's, Hughes Aircraft Company Electron Dynamics Division Applications Note, 1983.

20 H. G. Kosmahl, Modern multistage depressed collectors - A review, *Proc. IEEE Trans. Electron Devices*, Vol. 70, No. 11, pp.1325-1334, 1982.

21 J. T. Mendel, C. F. Quate and W. H. Yocom, Electron Beam focusing with periodic permanent magnet fields, *Proc. IRE*, pp. 800-810, May 1954.

22 J. W. Gewartowski and H. A. Watson, *Principles of Electron Tubes,* New Jersey: D. Van Nostrand Company, Inc., pp. 349-370, 1965.

23 J. D. Wilson, Traveling-wave thermionic devices, In T. Koryu Ishii's *Handbook of Microwave Technology, Volume 2*, pp. 57-95, San Diego: Academic Press, Inc, 1995.

24 J. R. Pierce, *Traveling-Wave Tubes*, New York: Van Nostrand, pp. 5-18, 1950.

25 B. Hantman, J. LaBelle, K. Siarkiewicz and R. Abrams, The MMACE framework: an integrated environment for power tube design and analysis, *Proc. Microwave Tubes for Space, Military and Commercial Applications Workshop,* Noordwijk, The Netherlands, April 1997.

26 W. B. Herrmannsfeldt, Electron trajectory program, Stanford Linear Accelerator Center Rep. 331, Stanford Univ., Stanford, CA, 1988.

27R. True, Electron beam formation, focusing, and collection in microwave tubes, In T. Koryu Ishii's *Handbook of Microwave Technology, Volume 1*, pp. 497-567, San Diego: Academic Press, Inc, 1995.

28 K. Nguyen, G. D. Warren, L. Ludeking and B. Goplen, Analysis of the 425-MHz klystrode, *IEEE Trans. Electron Devices,* Vol. 38, No. 10, pp. 2212-2220, October 1991.

29 J. Verboncoeur et. al., Comp. Phys. Comm. 87, 199, 1995.

30 C. L. Kory and J. D. Wilson, Three-dimensional simulation of traveling-wave tube cold-test characteristics using MAFIA, *NASA TP-3513*, May 1995.

31 C. L. Kory and J. D. Wilson, Simulation of cold-test parameters and rf power characteristics for a coupled-cavity traveling-wave tube, *IEEE Trans. on Electron Devices,* Vol. 42, No. 10, pp.2015-2020, November 1995.

32 C. L. Kory, Three-dimensional simulation of helix traveling-wave tube cold-test characteristics using MAFIA, *IEEE Trans. on Electron Devices*, Vol. 43, No. 8, pp. 1317-1319, August 1996.

33 C. L. Kory, J. D. Wilson and J. W. Maruschek, Simulation of cold-test dispersion and interaction impedance for coupled-cavity traveling-wave tube slow-wave circuits, *IEEE Int. Electron Devices Meet. Tech. Dig.*, pp. 763-766, 1992.

34 C. L. Kory, J. D. Wilson and J. W. Maruschek, Simulation of cold-test dispersion and interaction impedance for coupled-cavity traveling-wave tube slow-wave circuits, *IEEE Int. Electron Devices Meet. Tech. Dig.*, pp. 763-766, 1992.

35 J. W. Maruschek, C. L. Kory and J. D. Wilson, Generalized three-dimensional simulation of ferruled coupled-cavity traveling-wave tube dispersion and impedance characteristics, *NASA TP-3389*, November 1993.

36 B. Stockwell, K. Doniger and F. Friedlander, Advanced software coldtest of electron devices with μSOS, *IEEE Int. Electron Devices Meet. Tech. Dig.*, pp. 207-210, 1989.

37 A. A. Mondelli, J. J. Petillo and H. P. Freund, Cold-test and interaction models for helix TWT's in MMACE, *Proc. IEEE Int. Conf. on Plasma Science (ICOPS),* pp. 198-199, 1997.

38 K. D. Ward and J. Wlodarczyk, Transmission line modeling of helix slow-wave structures, *IEEE Int. Electron Devices Meet. Tech. Dig.*, pp. 157-160, 1993.

39 K. Halbach and R. F. Holsinger, Superfish-A computer program for evaluation of RF cavities with cylindrical symmetry, *Part. Accel.*, Vol. 7, pp. 213-222, 1976.

40 R. T. Benton, J. T. Burdette, J. A. Davis, J. R. Feicht, D. S. Komm, W. L. Menninger, N. R. Robbins, C. B. Thorington, X. Zhai and E. A. Adler, Efficiency improvements in KU-band space helix traveling-wave tubes, *Proc. Microwave Tubes for Space, Military and Commercial Applications Workshop,* Noordwijk, The Netherlands, April 1997.

41 C. L. Kory and A. H. Qureshi, Simulation of TunneLadder traveling-wave tube input/output coupler characteristics using MAFIA, *NASA CR-198505*, September 1996.

42 J. A. Dayton, Jr., H. G. Kosmahl, P Ramins and N. Stankiewicz, Analytical prediction with multidimensional computer programs and experimental verification of the performance, at a variety of operating conditions, of two traveling-wave tubes with depressed collectors, *NASA TP-1449,* May 1979.

43 K. R. Vaden, V. O. Heinen and J. A. Dayton, Jr., Three dimensional modeling of multistage depressed collectors, *Proc. IEEE Int. Conf. on Plasma Science (ICOPS),* p. 198, 1997.

44 L. Ludeking and J. Geary, C3D, A three-dimensional tool for collector design, *Proc. 1996 Microwave Power-Tube Conference*, May 1996.

45 K. D. Ward, M. J. Duffield and A. R. Wise, Power-booster traveling-wave tubes, *Proc. Microwave Tubes for Space, Military and Commercial Applications Workshop,* Noordwijk, The Netherlands, April 1997.

46 L. Kumar, P. Spädtke, R. G. Carter and D. Perring, Three-dimensional simulation of multistage depressed collectors on micro-computers, *IEEE Trans. on Electron Devices*, Vol. 42, No. 9, pp. 1663-1673, September 1995.

47 J. E. Rowe, *Nonlinear Electron-Wave Interaction Phenomena*, New York: Academic Press, 1965.

48 T. M. Antonsen and B. Levush, CHRISTINE, A multifrequency simulation code for traveling-wave tube amplifiers, *NRL Report*, 1996.

49 H. P. Freund and E. G. Zaidman, GATOR: A 3D time-dependent simulation code for helix TWT's, *Proc. IEEE Int. Conference on Plasma Science (ICOPS)*, p. 197, 1997.

50 H. K. Detweiler, Characteristics of magnetically focused large-signal traveling-wave amplifiers, Rome Air Development Center Tech. Rep. RADC-TR-68-433, Griffiss Air Force Base, NY, 1968.

51 J. D. Wilson, Revised NASA axially symmetric ring model for coupled-cavity traveling-wave tubes, NASA TP-2675, 1987.

52 F. Friedlander, A. Karp, B. Gaiser and B. Goplen, Transient analysis of beam interaction with antisymmetric mode in truncated periodic structure using three-dimensional computer code "SOS", *IEEE Trans. on Electron Devices*, Vol. ED-33, No. 11, pp. 1896-1901, 1986.

53 C. Smith, C. Armstrong, J. Duthie, G. Pierce and M. Sievers, MPM technology - The miniaturized transmitter solution, *Proc. Microwave Tubes for Space, Military and Commercial Applications Workshop*, Noordwijk, The Netherlands, April 1997.

54 R. L. Spence, Lewis investigates frequency sharing between future NASA space systems and local multipoint distribution systems in the 27-GHz band, Research and Technology 1996. NASA TM-107350, pp. 130, 1997.

55 J. A. Dayton, Jr. and G. H. Stevens, Commercial Opportunities for Microwave Tubes, 1996 Crane Microwave Tube Conference, Bloomington, Indiana, November 1996.

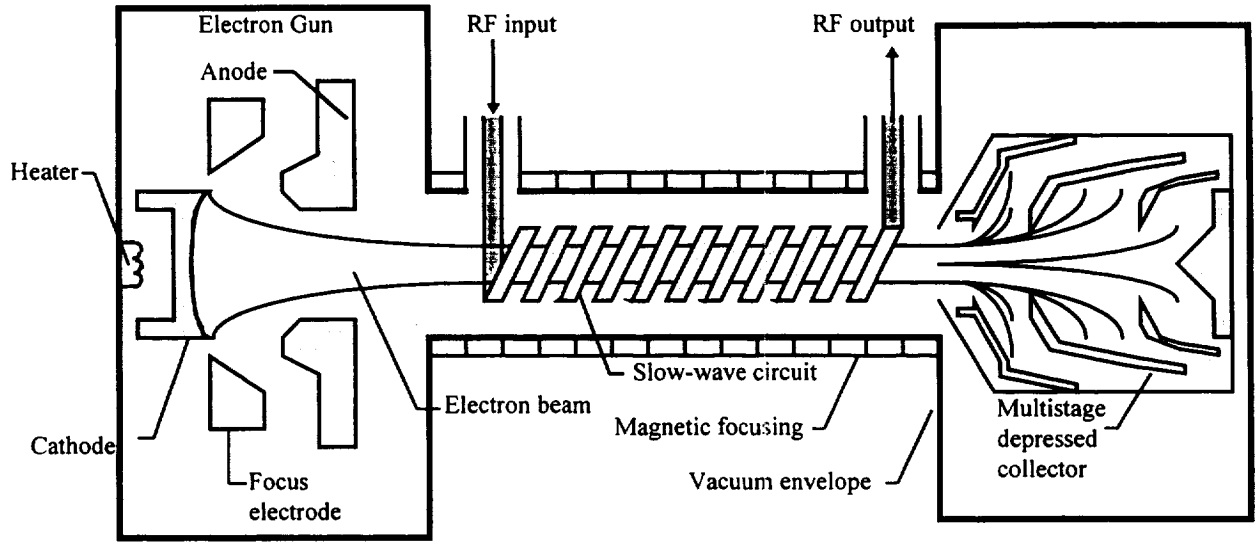

3178fg01.DOC

Figure 1

3178fg02.DOC

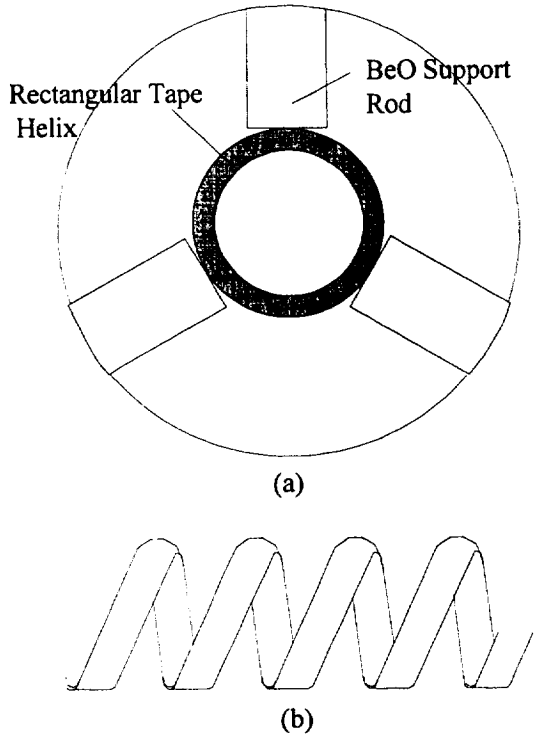

Figure 2 (a) Cross-sectional view of typical helix slow-wave circuit and (b) three-dimensional view of helical tape

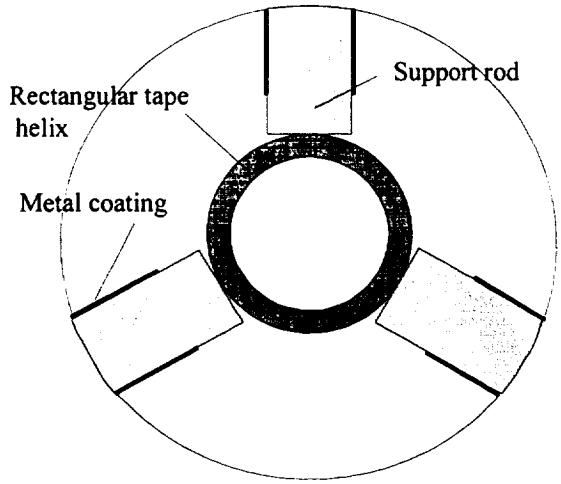
Support rod
Rectangular tape helix
Metal coating

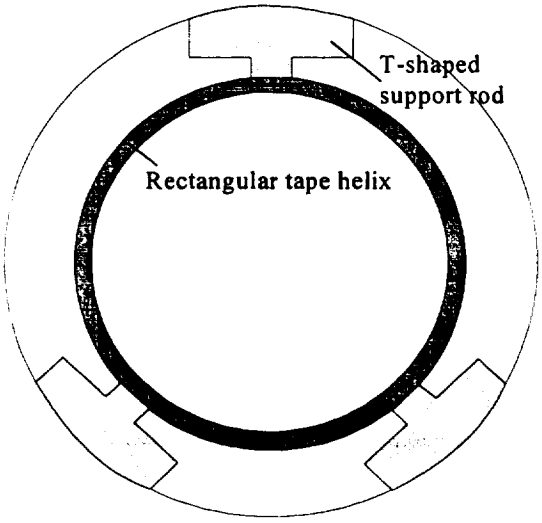
T-shaped support rod
Rectangular tape helix

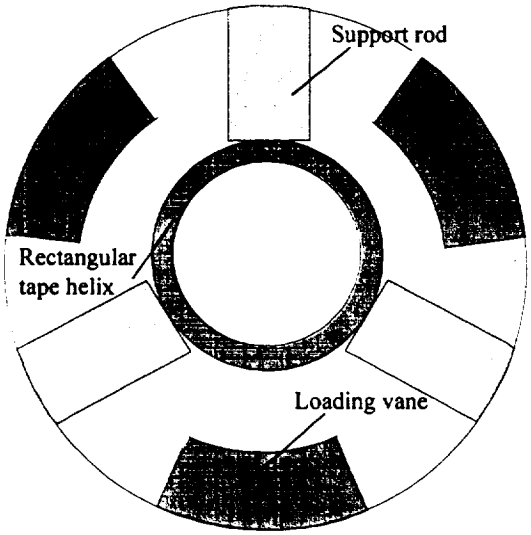
Support rod
Rectangular tape helix
Loading vane

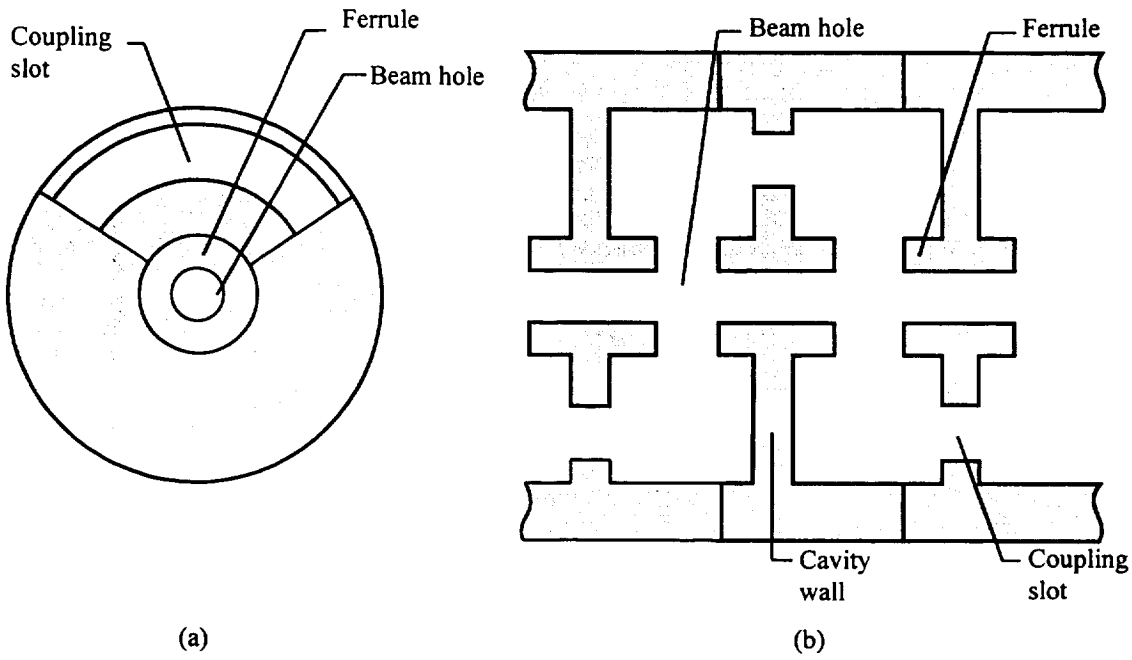

Figure 4 (a) Cross-sectional view and (b) top view of ferruled coupled-cavity circuit

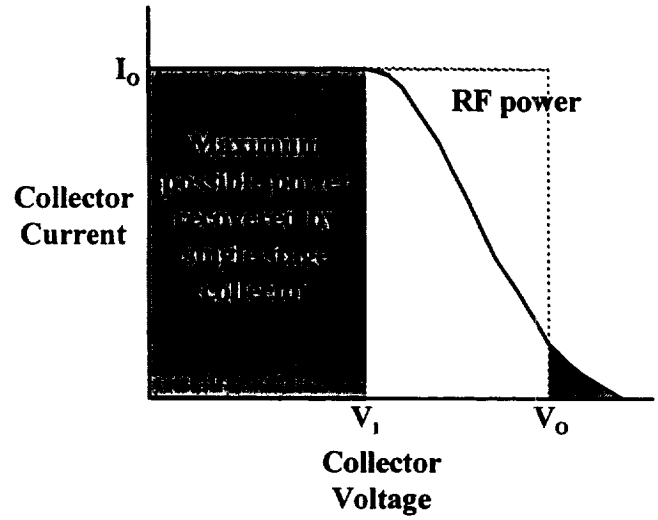
I_O
RF power
Collector Current
V_1
V_O
Collector Voltage

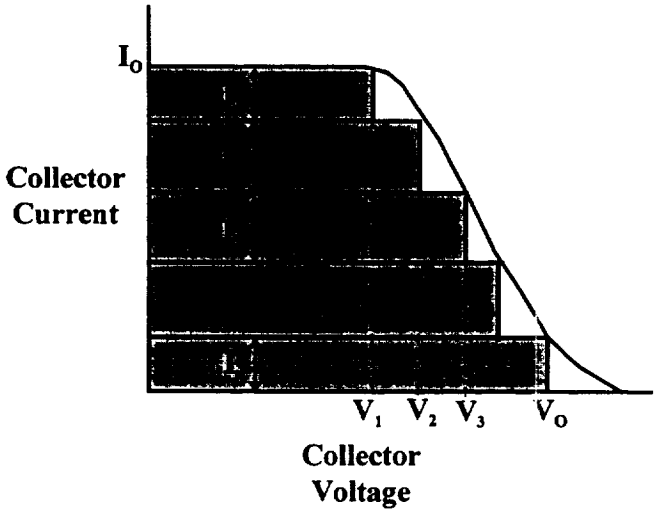
I_O
Collector Current
V_1
V_2
V_3
V_O
Collector Voltage

Figure 5

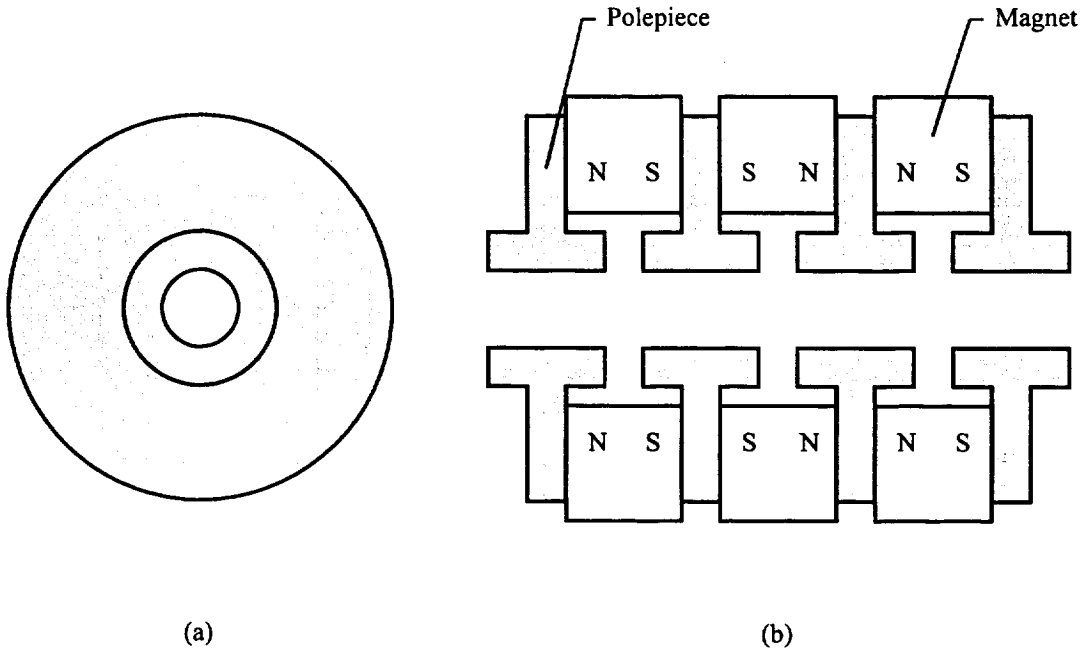

3178fg06.DOC

Figure 6 (a) Cross-sectional view and (b) top view of periodic permanent magnet focusing